AIP Advances

Properties of adsorbed supercritical methane film in nanopores

Cite as: AIP Advances **8**, 125011 (2018); https://doi.org/10.1063/1.5074086
Submitted: 21 October 2018 . Accepted: 04 December 2018 . Published Online: 12 December 2018

Jimmy Romanos, Sara Abou Dargham, Roy Roukos, and Peter Pfeifer

Properties of adsorbed supercritical methane film in nanopores

Jimmy Romanos,[1,a] Sara Abou Dargham,[1] Roy Roukos,[1] and Peter Pfeifer[2]
[1]*Department of Natural Sciences, Lebanese American University, Byblos, P.O.Box 36, Lebanon*
[2]*Department of Physics, University of Missouri, 223 Physics Building, Columbia, Missouri 65201, USA*

(Received 21 October 2018; accepted 4 December 2018; published online 12 December 2018)

Adsorbed natural gas technology is an efficient technology for storing natural gas at low pressure and room temperature. This work investigates the properties of the adsorbed methane film in nanopores where methane is adsorbed by strong van der Waals forces in pores of few molecular diameter as a high-density fluid. BET surface area, porosity, and pore size distribution were measured using sub-critical nitrogen adsorption. The adsorbed film thickness, the film density, specific surface area, and methane average binding energy were extracted from a single supercritical methane adsorption isotherm using Langmuir and Ono-Kondo models. In addition, this method does not require a conversion between gravimetric excess adsorption and absolute adsorption. The adsorbed film thickness is between 4.2 and 4.4 Å and the density of the adsorbed film at maximum capacity is between 302 and 340 g/L. Specific surface areas obtained from supercritical isotherms are consistent with BET surface areas from subcritical nitrogen adsorption. The binding energies obtained from the two models are compared to the ones obtained from Clausius-Clapeyron method.
https://doi.org/10.1063/1.5074086

I. INTRODUCTION

Storing natural gas (NG) by adsorption offers several advantages over exiting technologies. Liquefied natural gas (LNG) and compressed natural gas (CNG) have drawbacks when applied in the automotive industry and the petroleum industry. For instance, LNG requires heavy and expensive tanks, liquefaction and even with the best available insulators, a significant percentage of NG is lost by evaporation. On the other hand, CNG takes up considerable space and requires multi-stage compression. Adsorbed natural gas (ANG) is an alternative technology to store NG at low pressure.[1–6] Thermal management, cycling efficiency, sorbent packing, stability, and cost are currently hindering the widespread market adaptation of ANG.

The Advanced Research Projects Agency-Energy (ARPA-E) of the United States Department of Energy (DOE) has initiated a research program known as MOVE: Methane Opportunities for Vehicular Energy. The program aims to develop adsorbents for natural gas storage at low pressure and room temperature. The DOE has defined metrics to assess sorbents performance; the target for gravimetric storage density is 0.5 g/g and the target for volumetric energy density is 12.5 MJ/L. Activated Carbon (AC), Covalent Organic Frameworks (COFs), and Metal-Organic Frameworks (MOFs) are the leading materials used for adsorbed natural gas storage; reaching approximately 50 % of the gravimetric storage target and 75 % of the volumetric storage target.[7–13] Most research in the field focuses on increasing the gravimetric and volumetric storage capacities by increasing the surface area, optimizing the pore structure and the binding energy. This work propose assess several methods and propose alternative technique to study supercritical methane isotherms.

[a]Electronic mail: jimmy.romanos@lau.edu.lb

The binding energy of methane on adsorbent is usually determined using two isotherms at nearby temperatures using Clausius-Clapeyron equation. However, this method requires a conversion from excess to absolute adsorption by assuming or computing the volume of the adsorbed film.[14] Firlej et al. proposed a method to determine the high-coverage binding energy using a single isotherm and the pore-size distribution.[15] In this work, the average binding energy at low coverage and the overall average binding energy are extracted from supercritical methane adsorption isotherms. In addition, the specific surface area, the adsorbed film thickness, and the film density at maximum capacity are determined using the Ono-Kondo and Langmuir models.

II. EXPERIMENTAL

A. Materials

Sample "3K" is prepared from corncob biomass in a multi-step process consisting of phosphoric acid activation at 480 °C, followed by potassium hydroxide activation at 800 °C in a nitrogen environment. The partially activated carbon "HS;0B" is synthesized by the pyrolysis of polyvinylidene chloride. Further details of the synthesis and characterization of these materials is provided by Romanos and Olsen.[16–18] A commercial high-surface area carbon Maxsorb MSC-30,[19,20] produced by Kansai Coke and Chemical Co. Ltd, have been selected as a reference material for this study.

B. Sub-critical nitrogen adsorption at 77 K

Nitrogen adsorption isotherms were measured on an Autosorb instrument (Quantachrome). The total pore volume (V_{tot}) is measured at a pressure of 0.995 P/P_0 while the specific surface area Σ is measured using the Brunauer-Emmett-Teller (BET) theory in the pressure range of 0.01 to 0.03 P/P_0, which is suitable for nanoporous activated carbon. The intragranular porosity is calculated as follows:

$$\phi = \left[1 + \left(\rho_{skel}\frac{V_{tot}}{m_s}\right)^{-1}\right]^{-1} \tag{1}$$

Where ρ_{skel} is the skeletal density of the sample, assumed to be 2.0 g/cm^3. Typical skeletal densities of amorphous carbons are between 1.8 and 2.1 g/cm^3.[21] The porosity ϕ is calculated from the total pore volume (Vtot) using equation (1).

$$\rho_{app} = \rho_{skel}(1 - \phi) \tag{2}$$

The apparent density ρ_{app} is determined using equation (2). Quenched solid density functional theory (QSDFT) is used to calculate pore size distributions (PSDs). A detailed description of QSDFT has been published in a previous studies.[22,23]

C. Methane adsorption

Methane molecules are adsorbed by van der Waals forces in pores of few molecular diameter as a high-density fluid. The performance of a sorbent material is assessed by measuring an excess adsorption isotherm and converting it into volumetric and gravimetric storage capacities. The gravimetric excess adsorption G_e (g/kg) is determined by a volumetric measurement at 0 °C and 25 °C on custom-built automated Sieverts-type apparatus described extensively in literature.[24]

The gravimetric storage capacity G_s (g/kg) is calculated from the excess adsorption using the intragranular porosity of the sample determined from sub-critical nitrogen isotherms at 77 K. The volumetric storage capacity is determined by multiplying the gravimetric storage capacity by the apparent density.

$$G_s = G_e + \frac{\rho_{gas}}{\rho_{skel}}\left(\frac{\phi}{1-\phi}\right) \tag{3}$$

$$V_s = G_s \cdot \rho_{app} \tag{4}$$

III. THEORY

The determination of the specific surface area from experimental supercritical Langmuir isotherm has been done previously.[25] This method works for any adsorbate and it is based on the fact that, at high pressure and supercritical temperature, there is a complete monolayer coverage and absence of multilayer adsorption. The excess adsorption is defined as the mass of the adsorbed film minus the mass of an equal volume of gas at the corresponding pressure and temperature.

$$G_e(P,T) = \frac{m_{film}(P,T)}{m_s} - \frac{V_{film} \cdot \rho_{CH4}(P,T)}{m_s} \tag{5a}$$

$$\frac{m_{film}(P,T)}{m_s} = \frac{\chi(T) \cdot P}{1 + \chi(T) \cdot P} \frac{m_{CH4} \cdot \Sigma}{\alpha(T)} \tag{5b}$$

$$V_{film} = m_s \cdot \Sigma \cdot k \cdot \sqrt{\alpha(T)} \tag{5c}$$

Where $\alpha(T)$ is the area per adsorption site $\left(m^2\right)$, it is compared to the one from the fluid-fluid Lennard-Jones potential modeling parameter. For methane $\alpha(T) = \sigma^2{}_{CH4-CH4} = 0.145$ Å^2.[26,27] k = 1.075 is the packing factor for hexagonal packing,[25] $\chi(T)$is the Langmuir parameter $\left(bar^{-1}\right)$, Σ is the specific surface area $\left(m^2/g\right)$, V_{film} is the volume of the adsorbed film $\left(m^3\right)$, m_{CH4} is the mass of methane molecule (kg), and m_s is the mass of the sample (kg)

Dividing equation (5b) and (5c) will lead to the following equation:

$$\rho(P,T) = \frac{\chi(T) \cdot P}{1 + \chi(T) \cdot P} \cdot \frac{m_{CH4}}{k\alpha(T)^{\frac{3}{2}}} \tag{5d}$$

With increasing pressure, the excess adsorption reaches a maximum at P_{max}. As the pressure is increased further, the excess adsorption decreases since the density of the gas phase gradually approaches that of the adsorbed phase. The excess adsorption becomes zero at a pressure P_0, when the density of the adsorbed film is equal to the density of the bulk gas. We express P_0 as a function of T, k, and $\alpha(T)$ in the following equation:

$$P_0 = \frac{\mathrm{KT}}{\mathrm{k} \cdot \alpha(\mathrm{T})^{\frac{3}{2}}} \tag{5e}$$

Replacing (5b), (5c), (5d), and (5e) in equation (5a) will lead to the following equation:

$$G_e(P,T) = \frac{m_{CH4} \cdot \Sigma}{\alpha(T)} \left(\frac{\chi(T) \cdot P}{1 + \chi(T) \cdot P} - \frac{P}{kP_0} \right) \tag{6}$$

Methane adsorption is localized at room temperature. In localized adsorption, the adsorbed molecule has three vibrational degrees of freedom and oscillates around a minimum of the potential V (x, y, z) (adsorption potential) where z is the coordinate perpendicular to the surface, and x, y are the coordinates parallel to the surface. The vibrational frequencies in the three directions (ν_x, ν_y, ν_z) are usually of the order of 10^{12}.[14] Langmuir parameter $\chi(T)$is given by the following equation:[28]

$$\chi(T) = \frac{e^{\frac{E_B}{N_A KT}}}{\sinh\left(\frac{h\nu_x}{2KT}\right) \sinh\left(\frac{h\nu_y}{2KT}\right) \sinh\left(\frac{h\nu_z}{2KT}\right)} \sqrt{\frac{h^6}{(8\pi m)^3 (\mathrm{KT})^5}} \tag{7a}$$

E_B is the binding energy (J/mol), N_A is Avogadro constant (mol^{-1}), k is the Boltzmann constant (J/K), T is the temperature (K), h is Plank's constant (J.s), ν are the vibrational frequencies in the x, y, and z direction (s^{-1}), and m is the mass of the sample (kg). The binding energy can be calculated from the following equation:

$$E_B = N_A KT \cdot \ln\left[\sinh\left(\frac{h\nu_x}{2KT}\right) \sinh\left(\frac{h\nu_y}{2KT}\right) \sinh\left(\frac{h\nu_z}{2KT}\right) \sqrt{\frac{(8\pi m)^3 (\mathrm{KT})^5}{h^6}} \right] \tag{7b}$$

Aranovich and Donohue extended the Ono-Kondo model to gas adsorption on activated carbon.[29,30] It was applied to supercritical fluid by Chahine *et al.*[31] and more recently by Gasem et al.[32] and Bi et al.[33] The excess adsorption, determined from solving the Ono-Kondo equations for slit shaped pores, has four parameters: energy of the adsorbate-adsorbate interaction $E_{CH4-CH4}$(K), energy of adsorbate-adsorbent interaction E(K), density of the adsorbed film at maximum capacity ρ_{mc} (g/ml),

and a prefactor C related to the capacity of the adsorbent for a specific gas. Aranovich and Donohue solved the Ono-Kondo equations which relate the density of each layer to the bulk density and found the following general equation for the excess adsorption. Moreover, by neglecting the gas-gas interaction, one can reduce the number of parameters to three.

$$G_e(P,T) = 2C\frac{1-w^n}{(1-w_1)\left(1+w_1^{n-1}\right)}\frac{1-\frac{\rho_{gas}(P,T)}{\rho_{mc}}\left(1-e^{\frac{E}{KT}}\right)}{1+\left(\frac{\rho_{mc}}{\rho_{gas}(P,T)}-1\right)e^{\frac{E}{KT}}} \tag{8a}$$

Where n is the number of layer in a slit of the microporous material. w_1 is a factor which is a function of three coordination number and the fluid-fluid interaction energy and other variables discussed in detail by Aranovich and Donohue. For n=2, the excess adsorption can be written as:

$$G_e(P,T) = 2C\frac{1-\frac{\rho_{gas}(P,T)}{\rho_{mc}}\left(1-e^{\frac{E}{KT}}\right)}{1+\left(\frac{\rho_{mc}}{\rho_{gas}(P,T)}-1\right)e^{\frac{E}{KT}}} \tag{8b}$$

The results binding energy determined from the two models is compared with the one obtained from Clausius-Clapeyron equation using isotherms at 0 °C and 25 °C. The conversion from excess to absolute adsorption is performed using the following equation.

$$G_a(P,T) = G_e(P,T) + \rho_{gas}(P,T)\cdot V_{film} \tag{9}$$

where V_{film} is the volume of the adsorbed film determined from equation (5c).

IV. RESULTS AND DISCUSSION

The BET surface areas from sub-critical nitrogen adsorption are 900, 2600, and 2800 m^2/g for HS;0B, MSC-30, and 3K respectively. In addition, the intragranular porosities are 0.52, 0.79, and 0.81 for HS;0B, 3K, and MSC-30 respectively. Figure 1 shows the pore size distribution obtained from QSDFT. HS;0B has narrow pores below 20 Å with a single peak at 7 Å. MSC-30 and 3K have a bimodal pore size distribution with approximately double the pores below 10 Å when compared to HS;0B. Moreover, the pores of MSC-30 are below 30 Å with maximums at 7 and 18 Å and the pores of 3K are below 40 Å with maximums at 7 and 15 Å. Sample 3K has the largest volume of nanopores (< 10 Å) while MSC-30 has the largest volume of pores between 10 and 30 Å.

Figure 2 shows the gravimetric excess adsorption of sample MSC-30, 3K, and HS;0B at room temperature. HS;0B has the lowest gravimetric excess adsorption due to its relative low surface area and porosity. While 3K has the largest excess adsorption below 50 bar, MSC-30 has the largest excess adsorption at high coverage. Chi-square Levenberg-Marquardt minimization algorithm was used to

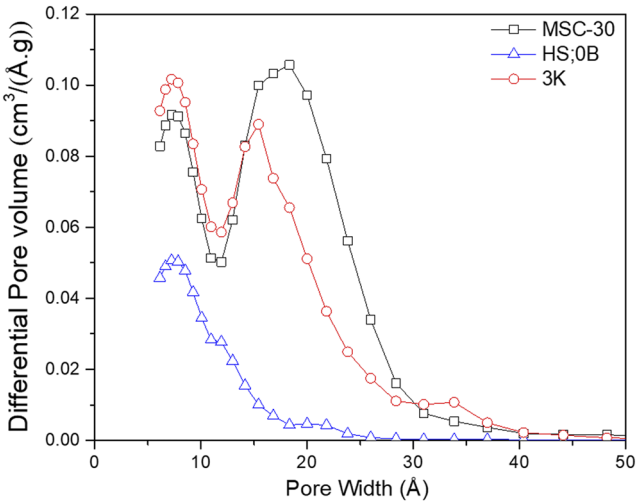

FIG. 1. Pore size distribution of 3K, MSC-30, and HS;0B from QSDFT.

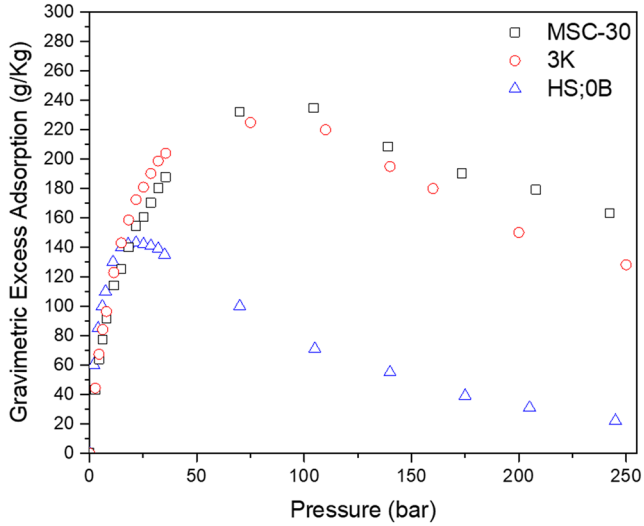

FIG. 2. Gravimetric Methane Excess Adsorption at 25 °C.

fit experimental excess adsorption with equation (6) for the Langmuir model and with equation (8b) for the Ono-Kondo model. Figure 3 shows the Langmuir and Ono-Kondo fit of experimental excess adsorption of MSC-30.

Table I provides the properties of the adsorbed film from Langmuir and Ono-Kondo fit. Both models provide a film thickness between 4.2 and 4.4 Å. The film thickness depends on adsorbate molecule. The density of the adsorbed film at maximum capacity is also comparable between the two methods. For HS;0B, the film saturation density is 319 g/L from Langmuir fit and 325 g/L from Ono-Kondo fit. For 3K, it is 308 g/L from Langmuir fit and 302 g/L from Ono-Kondo fit. As for the commercial carbon MSC-30, it is 340 g/L from Langmuir fit and 322 g/L from Ono-Kondo fit. These values are below 426 g/L, the density of liquid methane at the normal boiling temperature (112K). In addition, the Langmuir fit provides the specific surface areas from supercritical methane isotherm, which are comparable to the BET surface area obtained from subcritical nitrogen isotherm.

These two models provide the binding energies from a single isotherm. Most binding-energy determinations need two isotherms at nearby temperatures (Clausius-Clapeyron), and those are known

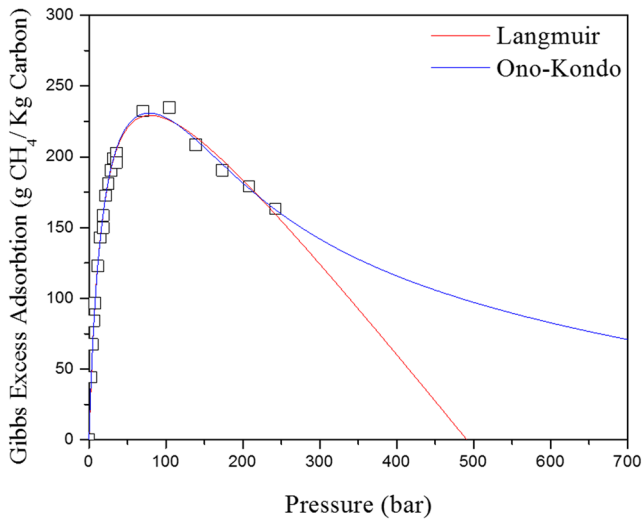

FIG. 3. Langmuir (red) and Ono-Kondo (blue) fits for the gravimetric excess adsorption.

TABLE I. Properties of the adsorbed film from supercritical methane isotherm.

		Film thickness (Å)	Density of the adsorbed film at maximum capacity (g/L)	Specific surface area from supercritical isotherm (m^2/g)	Average binding energy (kJ/mol)	Average binding energy at low-coverage (kJ/mol). Adsorption site active at P < 25 bar
HS;0B	Langmuir	4.4 ± 0.1	319 ± 9	751 ± 42	10.3 ± 0.3	16.7 ± 0.4
	Ono-Kondo	4.3 ± 0.1	325 ± 10	–	7.9 ± 0.2	14.6 ± 0.3
3K	Langmuir	4.2 ± 0.1	308 ± 7	2674 ± 156	13.1 ± 0.3	20.5 ± 0.4
	Ono-Kondo	4.2 ± 0.1	302 ± 7	–	9.7 ± 0.3	17.6 ± 0.4
MSC-30	Langmuir	4.4 ± 0.1	340 ± 11	2443 ± 137	12.2 ± 0.3	19.4 ± 0.4
	Ono-Kondo	4.4 ± 0.1	322 ± 9	–	8.9 ± 0.2	16.8 ± 0.3

to be tricky at high coverage because one needs good estimates of the film volume to construct accurate absolute adsorption isotherms. As a consequence, there exist only few accurate determinations of high-coverage binding energies (isosteric heats). The only other single-isotherm method to get an average or high-coverage binding energy requires the knowledge of the pore-size distribution.[15] The proposed models produce, from one single fit to one single excess isotherm, the average binding energy accurately. For HS;0B, the average binding energy is 10.3 kJ/mol from the Langmuir fit and 7.9 kJ/mol from the Ono-Kondo fit. For MSC-30, it is 12.2 kJ/mol from the Langmuir fit and 8.9 kJ/mol from the Ono-Kondo fit. As for 3K, it is 13.1 kJ/mol from the Langmuir fit and 9.7 kJ/mol from the Ono-Kondo fit. The results in the Ono-Kondo fits are more accurate since they do not involve the knowledge of the vibrational frequencies of methane. It is expected that Sample 3K has the largest average binding energy since it has the largest volume of pores below 10 Å. For instance, the adsorption potentials overlap in narrow pores resulting in a large binding energy. The average binding energy is consistent with the binding energy obtained from Clausius-Clapeyron equation. Figure 4 shows the binding energy calculated using Clausius-Clapeyron equation at 0 °C and 25 °C. The average binding energy is 9.4, 10.6, and 11.5 kJ/mol for samples HS;0B, MSC-30; and 3K respectively. In addition, the average binding energy at low coverage is obtained by fitting the excess adsorption at pressures below 25 bar. For HS;0B, the average binding energy at low coverage is 16.7 kJ/mol from the Langmuir fit and 14.6 kJ/mol from the Ono-Kondo fit. In addition, it is 19.4 kJ/mol from the Langmuir fit and 16.8 kJ/mol from the Ono-Kondo fit for MSC-30. For 3K, the average binding energy at low coverage is 20.5 kJ/mol from the Langmuir fit and 17.6 kJ/mol from the Ono-Kondo fit.

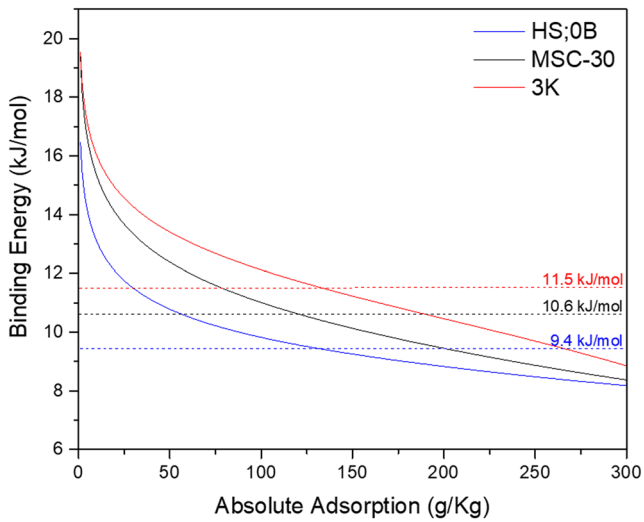

FIG. 4. Binding energy from Clausius-Clapeyron equation.

V. CONCLUSION

The adsorbed film thickness, the film density at maximum capacity, and specific surface area were determined from high pressure supercritical methane adsorption isotherm using Langmuir and Ono-Kondo models. The obtained surface area was consistent with the BET surface area obtained from subcritical nitrogen adsorption. This proposed method does not require a conversion between gravimetric excess adsorption and absolute adsorption. The adsorbed film thickness is 4.2-4.4 Å and the density of the adsorbed film at maximum capacity is 302-340 g/L. The average binding energies are consistent with the ones obtained from Clausius-Clapeyron equation.

ACKNOWLEDGMENTS

This work is supported in part by the Lebanese National Council for Scientific Research (Project number: 00752).

[1] T. K. Bose, R. Chahine, and J.-M. St-Arnaud, "High-density adsorbent and method of producing same" (1991).
[2] Y. Zhou, Y. Wang, H. Chen, and L. Zhou, Carbon **43**, 2007 (2005).
[3] Z.-L. Shi and Y.-B. Zhang, Israel Journal of Chemistry **0**.
[4] H. P. Kedar and S. Satyabrata, Journal of Natural Gas Science and Engineering **52**, 267 (2018).
[5] C. Kemp, B. B. Seung, L. Wang-Geun, M. Meyyappan, and S. K. Kwang, Nanotechnology **26**, 385602.
[6] M. Yuswan, G. Fiqi, and M. Mirza, IOP Conference Series: Earth and Environmental Science **105**, 012022.
[7] J. A. Mason, M. Veenstra, and J. R. Long, Chemical Science **5**, 32 (2014).
[8] Y. Peng, V. Krungleviciute, I. Eryazici, J. T. Hupp, O. K. Farha, and T. Yildirim, Journal of the American Chemical Society **135**, 11887 (2013).
[9] J. Jiang, H. Furukawa, Y.-B. Zhang, and O. M. Yaghi, Journal of the American Chemical Society **138**, 10244 (2016).
[10] F. Gándara, H. Furukawa, S. Lee, and O. M. Yaghi, Journal of the American Chemical Society **136**, 5271 (2014).
[11] K. C. Kemp, S. Bin Baek, W.-G. Lee, M. Meyyappan, and K. S. Kim, Nanotechnology **26**, 385602.
[12] J. Romanos, S. Sweany, T. Rash, L. Firlej, B. Kuchta, J. Idrobo, and P. Pfeifer, Adsorption Science & Technology **32**, 681 (2014).
[13] J. Romanos, T. Rash, S. A. Dargham, M. Prosniewski, F. Barakat, and P. Pfeifer, Energy & Fuels **31**, 14332 (2017).
[14] J. H. D. Boer (Clarendon Press, 1953) null.
[15] L. Firlej, M. Beckner, J. Romanos, P. Pfeifer, and B. Kuchta, The Journal of Physical Chemistry C **118**, 955 (2014).
[16] R. J. Olsen, A. K. Gillespie, C. I. Contescu, J. W. Taylor, P. Pfeifer, and J. R. Morris, ACS Nano **11**, 11617 (2017).
[17] J. Romanos, J. Burress, P. Pfeifer, T. Rash, P. Shah, and G. Suppes, "High surface area carbon and process for its production" (2016).
[18] T. Rash, A. Gillespie, B. Holbrook, L. Hiltzik, J. Romanos, Y. Soo, S. Sweany, and P. Pfeifer, Fuel **200**, 371 (2017).
[19] O. Toshiro, T. Ritsuo, and I. Masao, Gas Separation & Purification **7**, 241 (1993).
[20] H. Nishihara, P.-X. Hou, L.-X. Li, M. Ito, M. Uchiyama, T. Kaburagi, A. Ikura, J. Katamura, T. Kawarada, K. Mizuuchi, and T. Kyotani, The Journal of Physical Chemistry C **113**, 3189 (2009).
[21] D. R. Lide (CRC Press, 2005).
[22] A. V. Neimark, Y. Lin, P. I. Ravikovitch, and M. Thommes, Carbon **47**, 1617 (2009).
[23] P. I. Ravikovitch and A. V. Neimark, Langmuir **22**, 11171 (2006).
[24] R. Checchetto, G. Trettel, and A. Miotello, Measurement Science and Technology **15**, 127.
[25] G. Aranovich and M. Donohue, Journal of Colloid and Interface Science **194**, 392 (1997).
[26] W. A. Steele, *The interaction of gases with solid surfaces* (1974).
[27] Z. Tan and K. E. Gubbins, The Journal of Physical Chemistry **94**, 6061 (1990).
[28] J. Burress, M. Kraus, M. Beckner, R. Cepel, G. Suppes, C. Wexler, and P. Pfeifer, Nanotechnology **20** (2009).
[29] G. L. Aranovich and M. D. Donohue, Carbon **33**, 1369 (1995).
[30] G. L. Aranovich and M. D. Donohue, Journal of Colloid and Interface Science **180**, 537 (1996).
[31] P. Bénard and R. Chahine, Langmuir **13**, 808 (1997).
[32] M. Sudibandriyo, S. A. Mohammad, R. L. Robinson, Jr., and K. A. M. Gasem, Fluid Phase Equilibria **299**, 238 (2010).
[33] H. Bi, Z. Jiang, J. Li, F. Xiong, P. Li, and L. Chen, Energy & Fuels **31**, 2755 (2017).